Melt-mineral-fluid interaction in peralkaline silicic intrusions in the Oslo Rift, Southeast Norway. I: Distribution of elements in the Eikeren ekerite

E.-R. NEUMANN, T. ANDERSEN & T.H. HANSTEEN

Neumann, E.-R., Andersen, T. & Hansteen, T.H. 1990: Melt-mineral-fluid interaction in peralkaline silicic intrusions in the Oslo Rift, Southeast Norway. I: Distribution of elements in the Eikeren ekerite. *Nor. geol. unders. Bull. 417,* 1-13.

The behaviour of different elements during formation of the Eikeren ekerite (alkali granite) has been studied with the help of an element correlation matrix. The compositional relations are the result of partitioning of elements between a F-rich silicic melt, crystallizing phases (feldspar, sodic amphibole, acmitic pyroxene, sphene, apatite and ilmenite) and a Cl-F-rich fluid phase. The behaviour of the trace and minor elements Ba, Eu, Sm, Ca (and Sc) was governed by melt/crystal partitioning, and the melt/vapour distribution coefficients (D) were high. Also Cr, U and Rb were concentrated in the melt (D>1). Elements such as Zr, Hf, intermediate to heavy REE, Ta and Th were apparently stabilized in the fluid in F-complexes. D was slightly above 1 for Zr, Nb, and REE. Ni, Zn and Co appear to have had the lowest D-values (<1) in the system. Element transport by the fluid phase continued at subsolidus temperatures.

E.-R. Neumann, T. Andersen & T.H. Hansteen,
Mineralogisk-Geologisk Museum, Sarsgt. 1, 0562 Oslo 5, Norway.

Introduction

The Eikeren intrusive complex is the largest of a series of peralkaline granite complexes in the Permo-Carboniferous Oslo Rift (Fig. 1). The Eikeren ekerite was first described by Brøgger (1890), who originally called the rock 'soda granite', but later renamed it 'ekerite' (Brøgger 1906).

The complex has been dated by a Rb-Sr isochron to an age of 271±1 Ma, with an initial Sr isotope ratio of 0.7053±6 (Rasmussen et al. 1988). It thus represents some of the youngest igneous activity in the southern Oslo Rift where magmatism lasted from about 295 to 270 Ma ago (Sundvoll 1978, Rasmussen et al. 1988, Sundvoll, pers. comm. 1988).

Barth (1945) suggested that ekerite represents the end-product of the crystallization series kjelsåsite (monzodiorite)-larvikite (monzonite)-nordmarkite (alkali syenite)-ekerite. More recent studies have concluded that the ekerite formed from a volatile-rich 'residual' melt that was undergoing chemical fractionation as a result of mineral settling and loss of volatiles to the country-rocks (Dietrich et al. 1965, Neumann et al. 1977, Rasmussen et al. 1988).

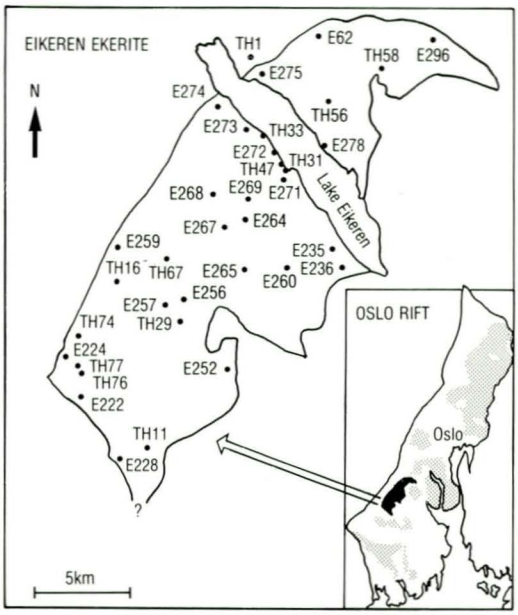

Fig. 1. Map of the Eikeren ekerite (alkali granite), showing sample localities and the position of the ekerite in the Oslo Rift. Based on maps by Brøgger & Schetelig (1926), Raade (1973), Ramberg (1976) and Andersen (1981).

This study was undertaken in order to evaluate the relative importance of crystallization and volatile transfer in controlling the behaviour of different elements during cooling of the Eikeren ekerite. The petrography and chemical analyses of fluid inclusions are presented in separate papers in this volume (Andersen et al. 1990, Hansteen & Burke 1990). A discussion based on bulk rock major and trace element data, and selected mineral chemical data, is presented below.

Petrography

Primary minerals

The Eikeren ekerite complex is texturally heterogeneous. The most abundant variety is a coarse-grained, miarolitic granite. Ekerite aplite is of minor abundance, but occurs both as inclusions in coarse-grained rocks and as dykes cutting these. The porphyritic ekerite contains subhedral alkali feldspar phenocrysts and sometimes rounded quartz grains in a granular quartz-feldspar matrix. Pegmatite occurs both in medium- to coarse-grained and aplitic ekerite. Different textural types may occur with clear age relations on the scale of a single outcrop (50-100m wide). However, it has not been possible to subdivide the pluton into separate units on a regional scale on textural or mineralogical criteria. The cross-cutting relations observed locally are therefore believed to reflect movements within the magma body rather than separate intrusions of magma.

Ekerite consists mainly of alkali feldspar and quartz. The most common accessory minerals are acmitic pyroxene, F-rich arfvedsonitic to richteritic amphibole, manganiferous ilmenite, magnetite with ilmenite lamellae (less common than ilmenite), zircon, sphene, F-apatite, astrophyllite and rutile. Primary, F-Fe-rich biotite (see below) occurs locally. The most common alteration products are chlorite, calcite, quartz, iron oxides, biotite, rutile/anatase and stilpnomelane(?).

Analytical data on amphiboles, clinopyroxenes and Fe-Ti-oxides from selected samples have been presented by Neumann (1974, 1976); additional amphibole analyses and representative analyses of biotite and chlorite are presented below.

The alkali feldspar is usually braid- or patch-perthite with almost equal amounts of microcline and albite. The grains are commonly covered by a rim of nearly pure albite composition. Cathodoluminescence images have revealed complex zoning patterns within each grain (this has been identified in terms of colour differences, red and blue, and so far not been quantified in terms of compositional variations). However, such differences have been described by Rae & Chambers (1988) and explained as the result of Fe-substitution (red) and lattice defects (blue). Granophyric intergrowths between alkali feldspar and quartz are common in samples with $SiO_2 > 72$ weight %. Zircon occurs both as euhedral, zoned grains and as a very late, interstitial to poikilitic phase.

The sodic amphibole is euhedral to subhedral, and occurs together with other accessory minerals in interstitial clusters (Fig. 2a), or as small euhedral inclusions in feldspar. Zoning is common. Larger grains of amphibole often carry inclusions of euhedral to subhedral Fe-Ti-oxides, zircon and apatite. In the same samples the amphibole has irregular contacts with feldspar and gives a general appearance of being partly resorbed. Intergrowths between sodic amphibole and sodic pyroxene are common.

The acmitic pyroxene (referred to below as acmite) is generally subhedral to anhedral (interstitial), and was one of the last minerals to start crystallizing. In some samples lacking sphene, however, acmite is euhedral (e.g. E252, TH1AB, TH77). Euhedral and subhedral acmite crystals are commonly zoned, and may have cores or zones consisting of a cryptic or symplectitic intergrowth between acmite and sodic amphibole, together with quartz and magnetite (e.g. samples E260, E269, TH77; Fig. 2b). Reverse zoning is also observed (sample E228). Experimental data on the stability of acmitic pyroxene and arfvedsonitic to

Fig. 2. Textural relations in ekerite. a: euhedral sodic amphibole (am) and interstitial acmite (p) in sample TH31 (a= apatite, o= Fe-Ti-oxide, q= quartz, f= alkali feldspar). b: euhedral acmite with cores which partly consist of intergrowths between acmite and sodic amphibole, and partly of quartz (sample TH77). c: quartz veinlet (indicated by arrows) with fluid inclusion trails representing a subsolidus fluid path (sample TH5C). d: alteration products after breakdown of amphibole, here along grain boudaries of feldspar (p= acmite, q= quartz, o= Fe-oxide, c= calcite, f= alkali feldspar) (sample TH33). Length of scale bar = 0.5 mm.


a
o
q
q
a


b


c
q

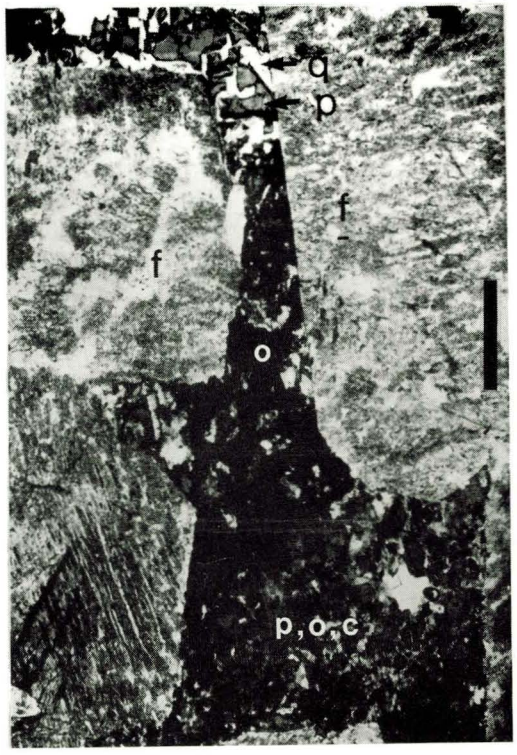
d
q
p
f
f
o
p, o, c

richteritic amphibole (Charles 1972, 1973, Ernst 1976) suggest that only small differences in oxygen fugacity are required to explain the observed differences in mode of occurrence of pyriboles.

This study has revealed (by microscopy and semi-quantitative microprobe analyses) a wide range of rare minerals occurring as primary magmatic phases: Y-niobates (fergusonite or euxenite), Ca-Na-niobates (pyrochlore or fersmite) and monazite occur as euhedral to subhedral grains. Y-fluorite is found partly as inclusions in euhedral acmitic pyroxene and Fe-Ti-oxides, and partly in interstitial aggregates of accessory minerals. Also, elpidite has been observed as an interstitial mineral. Light-REE F-carbonates such as synchisite and parisite occur in intimate intergrowths with opaque minerals and may represent alteration products. A detailed study of these minerals will be published separately. Such minerals have previously only been observed in miarolitic cavities and pegmatites in the Oslo Rift (Raade 1969, 1972, Raade & Haug 1980).

Secondary reactions

Evidence for secondary reactions is plentiful. Varying degrees of sericitization, 'swapped rims' between adjacent feldspar grains, and thin rims of albite on feldspar grains are observed in all samples.

In some samples, zones rich in fluid inclusions are found along recrystallized boundaries between quartz grains. These zones are generally also rich in Mn-rich ilmenite and may contain fluorite. An extreme example of this is sample TH5 which also shows veinlets of quartz with fluid inclusion trails cutting through primary grains of feldspar and quartz (Fig. 2c). The quartz in these veinlets has mainly grown in optical continuity with adjacent primary quartz grains, but does sometimes form a fine-grained aggregate. These observations are supported by cathodoluminescence images which show that what appear to be single grains of quartz under crossed nicols, in reality consist of light domains rimmed by, and cut by, dark domains. There is a clear correlation between quartz with low luminescence and trails of secondary, hydrous fluid inclusions. Hansteen & Burke (1990) found these inclusions to have formed at 300-400°C. The quartz veinlets and the zones rich in oxides thus appear to have been formed in connection with the transport of postmagmatic fluids through the system. The quartz in these zones may have recrystallized from primary grains, but the possibility that the system was open with respect to SiO_2 cannot be excluded.

In some samples, grains of amphibole are partly or totally replaced by a mixture of chlorite + calcite + iron oxide. Fe-oxide ± acmite + recrystallized quartz is commonly deposited in a skeletal configuration around the altered grain(s) (e.g. samples E228, E235, E236, E257, E265, TH27, TH33) (Fig. 2d). The reactions responsible may be of the following type (unbalanced)

1) $\underset{Na_{2.2}\ K_{0.3}\ Ca_{0.5}\ Mg_{2.3}\ (Mn,\ Fe)_{2.7}\ (OH)_{1.4}\ F_{0.6}\ Al_{0.3}\ Si_{7.7}O_{22}}{\text{Na-amph}} + CO_2 + H_2O + Al^{3+}$

$\rightarrow$ calcite + $\underset{Mg_{2.6}\ (Mn,\ Fe)_{2.2}\ Al_{2.1}\ (OH)_8\ Si_{3.0}O_{10}}{\text{chlorite}}$ + SiO_2 + Si^{4+} + Na^+ + K^+ + Fe^{2+} + F^+

Acmite ± Fe-oxide ± quartz is deposited as a skeletal growth outside the alteration regions, indicating that the fluid was saturated in Na.

Sphene is locally partly decomposed to calcite + quartz + rutile (or another TiO_2-oxide) (e.g. samples E245, TH33) according to the reaction

2) $CaTiO_5 + CO_2\,(fluid) = TiO_2 + SiO_2 + CaCO_3$.

Evidence of this reaction has also been observed in the Drammen biotite granite (Raade 1969). Schuiling & Vink (1967) have shown that, depending on the partial pressure of CO_2, this reaction will take place at temperatures ranging from 400 to 500°C.

The textures and reactions described above indicate that fluids continued to pass through these rocks at subsolidus temperatures. The observed reactions imply that the activity of H_2O and CO_2 in the fluid phase locally increased from magmatic to subsolidus temperatures. These fluids have clearly transported elements such as Na, K, Al, Fe, F and probably also Si. A detailed discussion of these fluids is presented by Hansteen & Burke (1990). Samples containing significant amounts of calcite are mainly found along the northern border of the ekerite complex, suggesting that the source of CO_2 may be the Cambro-Silurian carbonaceous sedimentary rocks.

Analytical methods

The size of a sample collected for chemical analyses was determined by its grain-size: coarse-grained samples > 5 kg, fine-grained samples 2-3 kg. Major elements were determined by X-ray fluorescence (XRF) analysis on a Philips instrument, using fused pellets made from rock powder mixed 1:9 with LiB_4O_7. The trace elements V, Cr, Ni, Zn, Rb, Sr, Zr, Ba and Pb were determined by XRF analysis (on a Philips instrument) on pressed powder pellets. The concentrations of other trace elements were obtained by instrumental neutron activation analysis methods described by Gordon et al. (1968) and Brunfelt & Steinnes (1969). All samples were analyzed in duplicate and calibrated against recommended values for international standards as given by Govindaraju (1984). Analytical precision estimated from duplicate analyses is listed in Table 1. International standards analyzed as unknowns give accuracies within the ranges of precision given in Table 1.

Table 1. Precision of analyses at the 1σ level of confidence.

Si, Al, Fe, Na, K, Rb, Sr (at 100 ppm), Zr	< ±1%
Ti, Mn, Ca, P (at 0.4 weight %), Sc, Zn, Cr	< ±2%
Mg, La, Sm, Th	±3%
Ba, Ce, Ta	±5%
Eu, Tb, Hf, U	< ±8%
Cs, Ni, Co	< ±11%
V, Lu	< ±15%
Yb, Pb	< ±20%

Mineral analyses were performed on an automatic Cameca Camebax microprobe with a wavelength dispersive system equipped with 3 spectrometers, using 15kV accelerating voltage and a sample current of 10nA. Standards were natural and synthetic minerals, and matrix corrections were made using the ZAF procedure in the Cameca software. Accuracy was frequently tested by analyzing standard minerals as unknowns.

Mineral analyses

Amphibole

Representative chemical analyses of amphiboles in the Eikeren ekerite are presented in Table 2. The amphiboles are of the F-richterite to F-arfvedsonite type, with high Na (6.8-10.3 weight %), Fe (14.3-25.4%), Mn (1.9-4.1%) and f (1.0-2.5%). Concentrations of CaO are low (<5.5%). Cl is below the detection limit.

The amphiboles are generally zoned, with increasing Fe, Mn and Na, and decreasing Al, Mg and Ca from core to rim (Table 2). F in amphibole shows a rough positive correlation with bulk rock SiO_2 (Fig. 3), but the zoning pattern is complex, with examples of both increasing and decreasing F from core to rim.

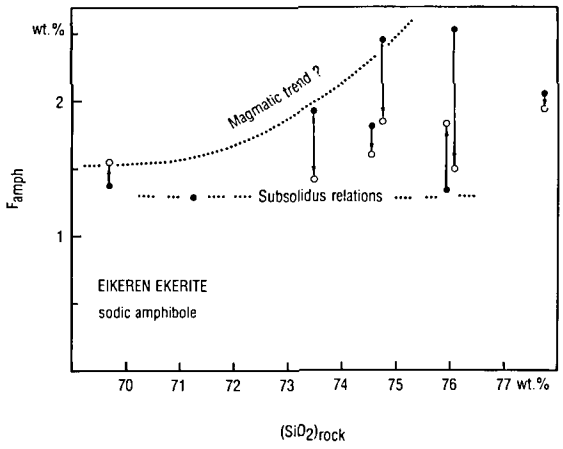

Fig. 3. Variations in F in amphiboles (F_{amph}) with bulk rock SiO_2. Closed circles = cores, open circles = rims, arrows show trends from core to rim within single samples. A magmatic trend of increasing F_{amph} with increasing bulk rock SiO_2 is schematically indicated (dotted line). See the text for further explanation.

Other minerals

Representative analyses of primary biotite and secondary chlorite are presented in Table 2. The biotite is rich in F, whereas Cl is close to the detection limit at about 0.02 weight %.

Table 2. Representative analyses of amphibole, biotite and chlorite (secondary) in the Eikeren ekerite. C = core, R = rim.

Wt. %	TH11C			TH29		TH31		TH33	TH56AG		TH56AI		TH74I		TH76AG		TH77		TH56AI	TH33
Amph.	6 C	5 C	5 R	C	R	C	R	Mean	C	R	C	R	C	R	C	R	Euhedr.	Anhedr.	Biotite	Chlorite
SiO_2	53.08	51.53	51.23	52.34	52.75	51.24	52.25	51.78	52.59	53.08	53.76	53.79	53.14	52.23	53.22	53.54	51.40	51.24	41.50	29.01
TiO_2	0.59	0.69	0.78	0.70	0.93	0.56	0.45	0.74	0.60	0.55	0.19	0.22	0.67	1.53	0.77	1.05	1.09	1.14	1.99	0.03
Al_2O_3	1.08	1.11	0.92	0.73	0.49	1.71	1.34	1.47	1.18	0.87	1.03	2.61	1.40	0.55	0.44	0.50	1.04	0.85	9.51	17.02
FeO_{total}	19.43	20.95	25.77	19.53	22.16	18.03	17.86	18.62	20.74	20.50	14.49	14.35	17.59	24.45	21.51	21.09	24.35	25.35	14.81	23.06
MnO	3.10	2.92	4.09	2.16	2.51	3.48	3.56	3.40	2.45	2.51	1.95	1.89	2.25	3.09	3.43	3.32	3.07	2.44	0.94	2.08
MgO	8.31	6.39	3.08	8.03	5.62	10.58	10.80	9.72	7.40	7.51	13.49	11.55	9.75	2.99	5.44	5.17	3.35	2.44	15.65	16.69
CaO	0.63	1.50	0.37	1.22	0.21	4.63	4.13	2.74	0.46	0.41	5.46	4.26	1.05	0.35	0.16	0.12	0.09	0.12	0.04	0.09
Na_2O	10.21	10.45	9.51	9.85	10.32	6.82	6.84	7.68	8.99	9.01	6.83	6.33	9.74	9.45	10.32	10.23	10.34	10.05	0.21	0.05
K_2O	0.97	1.10	1.27	1.20	1.42	1.04	1.08	1.14	1.19	1.27	1.01	1.05	1.06	1.53	1.40	1.55	1.43	1.64	9.26	0.03
F	2.25	2.53	1.50	2.46	1.85	1.37	1.55	1.29	1.81	1.62	1.68	0.97	1.93	1.43	2.06	1.95	1.83	1.55	2.56	0.06
Cl	<0.02	<0.02	<0.02	0.03	<0.02	<0.02	<0.02	0.02	<0.02	<0.02	<0.02	0.02	<0.02	<0.02	0.03	<0.02	<0.02	0.02	<0.02	0.03
Sum	99.67	99.19	98.54	98.25	98.28	99.48	99.88	98.60	97.43	97.35	99.91	97.04	98.60	97.62	98.78	98.54	98.01	96.84	96.49	88.15

Table 3. Compositional variations among ekerites in the Eikeren intrusive complex. For the TH samples, total iron is given as Fe_2O_3.

Wt. %	E62	E207	E222	E224	E228	E235	E236	E252	E256	E257	E259	E260	E264	E265	E267	E268	E269	E271	E272	E273	E274	E275
SiO_2	76.60	70.94	69.51	73.04	74.98	75.61	76.21	75.91	72.77	69.56	71.98	75.26	72.58	73.69	72.14	73.00	72.18	74.14	70.44	70.63	72.17	68.68
TiO_2	0.51	0.43	0.42	0.39	0.34	0.27	0.29	0.23	0.40	0.44	0.50	0.31	0.40	0.31	0.36	0.41	0.40	0.52	0.39	0.58	0.37	0.54
Al_2O_3	10.80	13.89	14.34	12.44	10.87	10.91	10.87	11.03	13.56	13.53	13.81	11.13	12.38	12.01	13.35	13.98	12.68	13.20	13.21	13.71	13.47	14.40
Fe_2O_3	2.16	3.85	1.60	1.90	2.11	2.33	2.31	2.08	2.13	1.85	2.04	2.17	2.26	2.18	1.86	1.68	2.10	2.10	1.70	2.11	1.13	2.02
FeO	0.58		0.72	0.70	0.55	0.73	0.58	0.47	0.38	0.77	0.81	0.50	0.59	0.27	0.40	0.52	0.63	0.92	0.89	1.48	1.16	0.92
MnO	0.17	0.15	0.10	0.14	0.14	0.11	0.16	0.16	0.17	0.12	0.12	0.13	0.17	0.21	0.10	0.14	0.14	0.19	0.12	0.19	0.09	0.13
MgO	0.00	0.21	0.12	0.05	0.02	0.00	0.00	0.00	0.03	0.07	0.10	0.39	0.08	0.00	0.05	0.40	0.13	0.55	0.13	0.42	0.07	0.22
CaO	0.11	0.44	0.28	0.22	0.10	0.10	0.00	0.03	0.15	0.20	0.26	0.18	0.16	0.00	0.07	0.33	0.32	0.60	0.38	0.52	0.27	0.48
Na_2O	3.34	4.92	5.31	4.77	4.04	4.08	3.94	3.87	4.56	5.03	5.01	4.38	4.76	3.95	4.94	5.45	5.06	5.30	5.21	5.53	4.96	5.53
K_2O	4.34	5.03	5.44	4.80	4.68	4.53	4.45	4.67	5.14	5.23	5.25	4.59	4.54	5.22	4.97	5.04	4.54	4.50	4.54	4.37	5.08	5.18
P_2O_5	0.02	0.08	0.05	0.04	0.02	0.01	0.01	0.01	0.03	0.04	0.06	0.00	0.04	0.02	0.03	0.03	0.05	0.10	0.06	0.10	0.04	0.03
H_2O	0.22	0.24	0.22	0.18	0.16	0.22	0.12	0.16	0.33	0.20	0.22		0.36	0.33	0.24		0.22	0.34	0.34	0.14	0.34	0.18
Sum	98.85	100.18	98.11	98.67	98.01	98.90	98.94	98.62	99.65	97.04	100.16	99.04	98.32	98.19	98.51	100.98	98.45	102.46	97.41	99.78	99.15	98.35
ppm																						
Sc		4.4										3.4				4.1		5.3		6.8		
Y	18	8	15	16	15	13	14	13	14	18	19	11	20	15	17	12	19	17	19	18	16	20
Cr	166	145	82	171	138	278	282	210	84	170	188	221	147	139	127	130	126	164	194	182	151	151
Co		3.3										1.0				0.7		1.3		1.4		
Ni	3.0		1.3	3.2	2.1	4.5	4.8	3.5	1.5	3.6	3.8		2.8	2.7	1.2		2.2		2.8	3.1	1.6	0.1
Zn	174		76	105	106	177	102	181	197	95	140		184	171	112		173		114	120	92	123
Rb	185	308	135	194	197	240	271	228	175	156	126	240	172	194	122	110	152	130	127	84	137	123
Sr	6	34	8	12	17	6	5	17	121	14	19	3	22	8	14	19	38	51	52	53	11	37
Zr	1016	1111	555	912	660	684	1304	723	701	770	706	1150	1047	1113	583	571	806	755	654	1030	320	767
Cs		1.9										0.8				0.7		0.6		0.4		
Ba	79	439	371	103	24	17	13	39	117	135	161	100	355	44	208	416	521	489	529	943	180	519
La		176								89		19				86		74		119		
Ce		345								221		110				209		166		173		
Sm		25.3								19.9		11.0				16.7		20.2		28.9		
Eu		1.7								3.2		1.6				3.2		4.0		7.1		
Tb		3.3								3.5		2.1				3.1		3.6		1.6		
Yb		13								14		17				5		14		10		
Lu		2.5								1.8		2.8				0.9		1.9		1.8		
Hf		36										43				18		23		19		
Ta		21.5										17.3				6.9		13.4		5.8		
Th	26.3	45.0	14.5	34.4	24.3	24.3	53.0	20.3	19.9	19.0	16.7	21.8	26.6	23.7	12.2	10.1	16.3	13.8	10.5	7.0	7.4	22.7
Pb	60		28	24	26	20	41	40	17	43	8		21	11	9		22		26	7	10	16
U	4.2	11.9	3.2	7.2	5.7	9.5	8.8	8.2	3.9	3.4	2.5	10.1	5.0	3.9	1.6	2.3	3.8	4.2	3.5	2.6	1.7	2.2

Wt. %	E278	E296	TH1AB	TH11AB	TH11C	TH13I	TH16A	TH29	TH31	TH33	TH47F	TH53	TH56AG	TH56A	TH58	TH67M	TH74I	TH76AG	TH77
SiO_2	72.81	72.76	76.54	71.04	76.14	72.17	65.40	74.75	69.73	71.25	70.19	73.05	74.53	65.96	77.84	75.80	73.48	77.73	75.95
TiO_2	0.28	0.35	0.27	0.54	0.19	0.49	0.87	0.36	0.57	0.40	0.65	0.37	0.40	0.79	0.15	0.34	0.13	0.11	0.19
Al_2O_3	12.93	12.26	12.40	13.22	11.18	13.47	15.78	12.99	14.38	14.40	13.45	14.12	13.03	14.72	11.80	12.03	14.33	9.53	10.90
Fe_2O_3	1.47	2.49	2.04	3.35	3.02	2.88	3.63	2.53	3.90	2.58	3.94	2.59	2.49	4.23	1.95	2.45	1.89	4.45	3.44
FeO	0.48	0.51																	
MnO	0.11	0.08	0.11	0.20	0.19	0.15	0.20	0.14	0.24	0.14	0.22	0.15	0.17	0.23	0.10	0.13	0.08	0.10	0.19
MgO	0.01	0.08	0.09	0.31	0.07	0.27	0.53	0.11	0.44	0.19	0.50	0.23	0.18	1.04	0.02	0.20	0.03	0.02	0.03
CaO	0.17	0.25	0.00	0.16	0.01	0.26	0.64	0.01	0.73	0.31	0.75	0.12	0.20	1.96	0.10	0.00	0.00	0.00	0.08
Na_2O	4.96	4.12	4.40	5.16	4.31	5.05	6.04	4.80	5.91	5.57	5.47	5.39	4.73	6.07	3.95	4.17	4.81	3.98	4.39
K_2O	4.79	4.67	4.75	5.25	4.45	5.00	5.44	4.89	4.14	4.58	4.12	4.59	4.35	4.78	4.38	4.69	5.53	4.29	4.41
P_2O_5	0.03	0.05	0.03	0.06	0.02	0.06	0.18	0.04	0.14	0.07	0.15	0.06	0.06	0.21	0.02	0.03	0.03	0.02	0.02
H_2O	0.33	0.24	0.09	0.33	0.10	0.13	0.13	0.16	0.16	0.27	0.26	0.24	0.32	0.36	0.25	0.22	0.17	0.05	0.16
Sum	98.37	97.86	100.72	99.62	99.68	99.93	98.84	100.78	100.34	99.76	99.70	100.91	100.46	100.35	100.56	100.06	100.48	100.28	99.76
ppm																			
Sc			3.0	6.6	4.2	5.2	10.3	3.6	6.2	4.2	6.6	4.3	4.0	8.6	3.5	3.3	2.3	1.4	5.2
Y	14	20	26	10	8	9	13	8	24	14	21	13	16	51	8	10	6	7	9
Cr	126	261	192	142	211	188	104	190	158	227	125	190	219	107	293	257	172	186	208
Co			1.8	2.1	3.5	2.0	1.7	2.3	3.2	1.9	2.9	1.9	2.8	5.4	2.2	2.5	2.2	1.9	2.5
Ni	0.9	4.0																	
Zn	83	113																	
Rb	159	179	183	186	225	139	121	196	124	105	122	133	137	198	210	203	238	376	285
Sr	6	7	4	6	3	9	34	6	109	51	79	31	38	87	28	4	6	2	3
Zr	477	799	207	733	1369	861	357	811	999	631	1210	632	630	394	221	735	728	281	709
Cs			1.4	0.7	2.4	0.5	0.8	1.2	0.8	2.3	0.5	0.9	0.8	0.8	1.5	1.0	4.2	1.2	2.7
Ba	81	348	78	206	73	301	472	173	680	698	603	536	468	454	106	118	103	33	96
La			43	150	33	111	106	71	76	74	91	69	69	72	19	62	14	25	61
Ce			87	297	105	241	207	160	239	138	197	171	144	138	48	169	69	60	123
Sm			4.6	15.5	10.1	19.7	18.7	16.4	21.1	20.4	24.2	15.9	18.2	17.7	2.8	17.7	7.9	8.6	10.1
Eu			0.7	2.4	1.7	3.3	3.8	2.7	5.0	4.8	5.4	3.7	3.7	3.3	0.4	2.5	1.7	1.1	1.5
Tb			0.6	2.3	2.3	1.7	1.3	2.0	2.0	1.7	2.7	1.4	1.9	1.6	0.5	2.0	3.0	1.0	1.7
Yb			3	12	12	9	5	9	11	6	12	8	7	7	4	9	12	5	10
Lu			0.7	2.3	2.5	1.6	0.9	1.7	2.1	1.2	2.3	1.4	1.5	1.3	0.9	1.8	2.2	1.1	2.0
Hf			7	27	50	22	11	25	29	17	36	18	21	13	10	22	43	14	12
Ta			6.2	13.7	24.1	9.1	4.7	10.2	10.9	6.6	13.5	7.3	10.8	3.9	6.5	12.0	7.6	10.8	15.9
Th	15.9	21.3	10.6	35.4	32.6	15.2	9.7	21.6	11.3	7.6	26.6	11.9	15.5	12.0	6.9	14.9	55.3	9.3	24.0
Pb	4	26																	
U	3.5	2.7	4.7	6.7	13.8	4.9	2.1	4.7	3.8	2.1	2.8	2.8	8.1	1.3	4.2	6.0	1.4	14.8	11.4

Analyzed apatite contains 2.6-3.8 weight % F, and no detectable Cl. Chemical data on apatites and other accessory phases will be presented separately.

Whole-rock compositional variations

The ekerites consist primarily of SiO_2 (69.2-76.6 weight %), Al_2O_3 (10.8-14.4%), Na_2O (3.3 - 5.7%) and K_2O (4.3-5.4%) Table 3). FeO_{total} is between 2.1 and 2.8%, whereas all other major elements are below 1%. The highest concentrations of TiO_2 are found in those samples which have most sphene.

When projected into the Q - Ab - Or system, the rocks fall in the low-pressure thermal valley in the feldspar field, with normative quartz ranging from 17 to 40 weight %. In the Si-Al-(Na+K) system, the rocks fall close to the line of division between the alkaline and

peralkaline fields (Fig. 4). The ekerites do not, however, define a trend of increasing peralkalinity with increasing Si. Such trends, which are interpreted as being due to removal of feldspar, are found in other Oslo Rift silicic complexes (e.g. Andersen 1984), and have been observed in several silicic volcanoes in the East African Rift System (Barberi et al. 1982).

The concentrations of trace elements vary considerably, and this is particularly true for the lithophile elements, e.g. La: 19-176 ppm, Ta: 4-24 ppm, Th: 7-55 ppm, and Rb: 83-376 ppm (Table 3, Fig. 5). The concentrations of Co and Ni are below 5 ppm, whereas those of Cr (82-282 ppm) are considerably higher than expected in highly silicic rocks.

Chondrite-normalized REE-patterns (Fig. 6) show a very variable light REE-enrichment and weak to strong negative Eu-anomalies. There is no correlation between the La/Lu ratio or the Eu-depletion, and the REE-concentration.

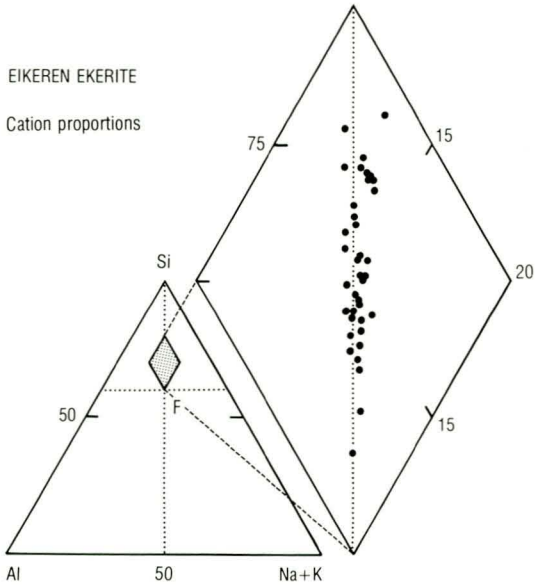

Fig. 4. Eikeren ekerite samples projected into the Si — Al — (Na+K) system. The ekerite samples plot along the dividing line (dotted, vertical) between the alkaline and the peralkaline fields.

Element correlation patterns

The textural relations described above and the fluid inclusion studies of Hansteen & Burke (1990) show that the formation of the Eikeren ekerite involved both crystallization and fluid transport. In order to determine the details of how these processes have governed the behaviour of different elements, it is necessary to study the entire geochemical data set. One way of doing this is to calculate a correlation matrix. Good correlations (that is correlation coefficients (R) close to +1.0 or +1.0) are expected if the chemical variations in a group of rocks are dominated by one process. A combination of processes would superimpose different correlation patterns on the rock chemistry, resulting in poor correlations (R close

Table 4. Major and trace element correlation coefficients (R) for the Eikeren ekerite. Underlined numbers belong to correlation groups discussed in the text. The samples TH1AB and TH56AI are excluded as they represents a dyke and a xenolith, respectively.

	Ba	Eu	Sm	Ca	Na	P	Mg	Al	Ti	Sr	Sc	V	La	Mn	Fe	Tb	Ni	Zn	Co	K	Yb	Zr	Lu	Hf	Ta	Th	Cs	Pb	Cr	U	Rb	Si
Ba	1																															
Eu	.94	1																														
Sm	.80	.94	1																													
Ca	.78	.76	.69	1																												
Na	.76	.80	.74	.76	1																											
P	.75	.73	.67	.89	.77	1																										
Mg	.69	.66	.66	.79	.67	.77	1																									
Al	.63	.63	.57	.60	.89	.67	.49	1																								
Ti	.61	.73	.78	.78	.66	.83	.71	.62	1																							
Sr	.59	.75	.63	.65	.48	.59	.45	.44	.46	1																						
Sc	.54	.56	.57	.73	.75	.83	.70	.63	.89	.47	1																					
V	.52	.80	.76	.63	.38	.46	.23	.33	.55	.46	.52	1																				
La	.52	.62	.74	.49	.68	.55	.53	.55	.78	.34	.72	.42	1																			
Mn	.32	.57	.56	.41	.21	.50	.50	.05	.49	.46	.77	.22	.58	1																		
Fe	.25	.22	.21	.32	.16	.46	.31	-.10	.29	.21	.38	.07	.27	.45	1																	
Tb	.02	.18	.29	.19	.25	.03	.25	.24	.15	.01	.00	.30	.15	.10	-.36	1																
Ni	-.02			.01	-.28	.02	.06	-.34	.05	-.22		.17		.13	.70		1															
Zn	-.11			-.28	-.44	-.27	-.19	-.40	-.07	.37		-.07		.57	.20		.18	1														
Co	-.13	-.06	-.09	-.09	-.17	.11	-.36	-.13	.13	.20	-.00	.11	.13	.33	.34	.13			1													
K	-.22	-.19	-.07	.12	.25	-.04	-.13	.52	.17	-.22	.20	-.12	.26	-.32	-.34	.30	-.30	-.29	-.33	1												
Yb	-.12	.07	.15	.09	.02	-.06	.21	-.08	.05	-.02	.02	.24	.00	.21	-.10	.62			.0	.06	1											
Zr	.05	.33	.36	.04	-.13	-.00	.12	-.21	.10	.08	.12	.23	.09	.52	.17	.42	.57	.36	.32	-.27	.74	1										
Lu	-.17	-.01	.04	-.01	-.11	-.11	.09	-.21	-.07	-.04	-.02	.11	-.07	.30	.08	.43			.32	-.09	.91	.83	1									
Hf	-.20	-.07	-.08	-.08	-.10	-.14	.03	-.09	-.15	-.06	-.18	.00	-.27	.08	-.08	.53			.32	.05	.76	.79	.83	1								
Ta	-.45	-.34	-.25	-.23	-.43	-.32	-.14	-.60	-.30	-.28	-.17	-.11	-.25	.28	.13	.30			.43	-.30	.63	.64	.74	.63	1							
Th	-.45	-.33	-.32	-.37	-.34	-.29	-.30	-.26	-.25	-.30	-.18	-.21	-.18	.06	-.04	.44	.54	.10	.31	.14	.52	.54	.65	.71	.42	1						
Cs	-.42	-.45	-.57	-.50	-.32	-.40	-.67	-.12	-.62	-.39	-.40	-.50	-.56	-.42	-.22	.07			.28	.25	.03	-.04	.15	.28	.13	.62	1					
Pb	-.30			-.33	-.55	-.39	-.35	-.55	-.02	-.22		-.16		.14	.09		.37	.13		-.28		.43				.48		1				
Cr	-.21	-.43	-.46	-.36	-.50	-.35	-.23	-.49	-.47	-.30	-.59	-.29	-.56	-.23	.00	-.45	.84	.02	.18	-.46	-.13	.10	-.04	-.08	.13	.13	.25		1			
U	-.48	-.56	-.49	-.45	-.55	-.44	-.25	-.77	-.51	-.34	-.38	-.47	-.40	.13	.38	-.24	.48	.29	.28	-.43	.10	.21	.28	.18	.73	.25	.12	.42	.41	1		
Rb	-.73	-.81	-.77	-.66	-.74	-.61	-.52	-.79	-.71	-.49	-.59	-.60	-.62	-.17	.22	-.25	.42	.30	.15	-.20	.02	.04	.16	.10	.41	.45	.44	.50	.41	.79	1	
Si	-.70	-.72	-.71	-.77	-.94	-.83	-.65	-.93	-.80	-.49	-.82	-.43	-.71	-.25	-.19	-.25	.20	.37	.12	-.41	-.03	.11	.11	.10	.45	.28	.31	.47	.55	.64	.75	1

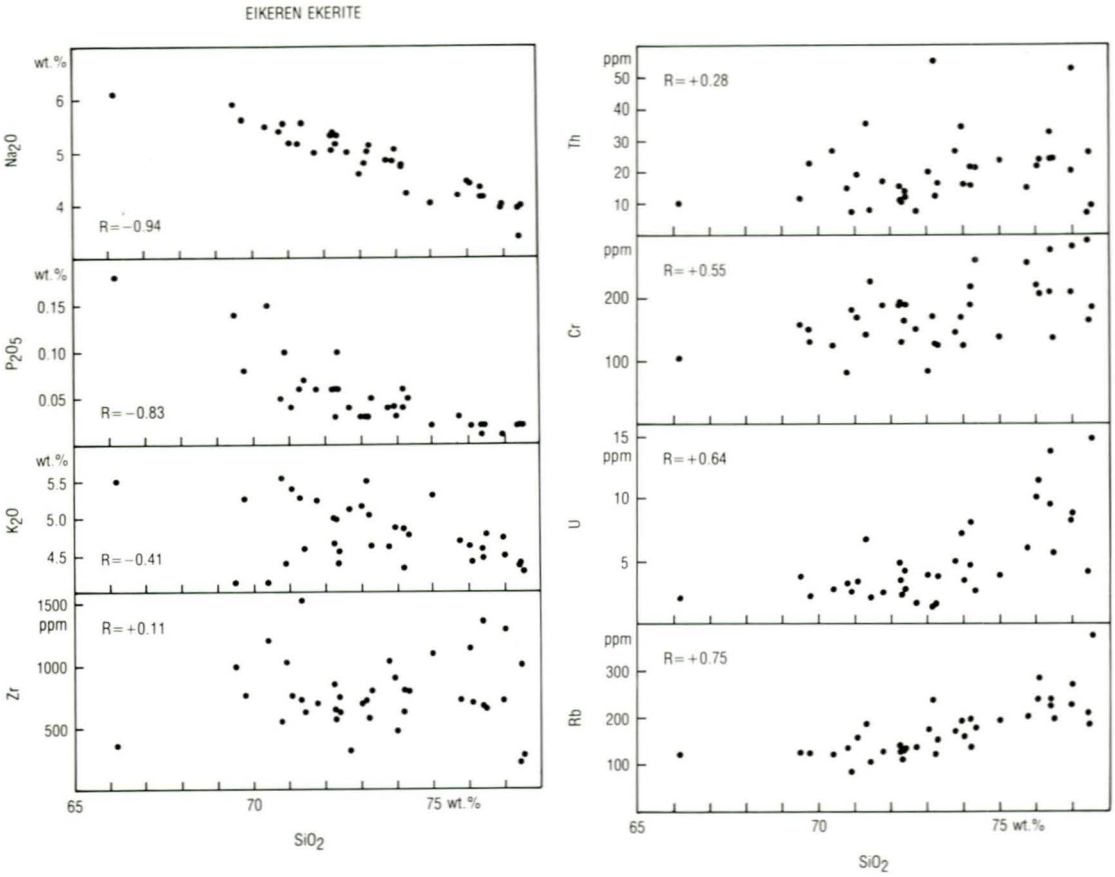

Fig. 5. The variations of selected elements relative to SiO2
R= correlation coefficient (see explanation in the text).

to 0.0). One problem, however, is that the estimated correlation coefficients are based on *linear* correlations; this means that well defined, broken or curved trends will also give poor R-values.

A correlation matrix for the Eikeren ekerite is presented in Table 4. The samples TH1AB and TH56AI are excluded from the samples in the data basis for the correlation matrix, as they represent a dyke and a xenolith, respectively. Som gaps occur in the matrix because some of the elements have been determined only for selected sets of samples. The elements in the correlation matrix are organized according to their correlation with Ba. Ba was chosen as a basis because it is a trace element preferentially entering alkali feldspar, which is a liquidus mineral in the ekerite. Some minor adjustments of the sequence of elements in Table 4 were made in order to group elements with strong internal correlations.

The elements Ba, Eu, Ca. Sm, Na, P, Mg, Al and Ti (Table 4) show strong negative correlations with Si ($R<-0.7$) and strong positive correlations with each other ($R> +0.6$). Examples are shown in Fig. 7. For simplicity this group of elements will be referred to as the *Ba-group*. The elements in the *Ba-group* are preferentially picked up by minerals which represent the primary phases in the Eikeren ekerite: alkali feldspar, sodic amphibole, (acmitic pyroxene), sphene, ilmenite, titanomagnetite and apatite (e.g. Neumann 1974, Mahood & Hildreth 1983, Wörner et al. 1983, Lemarchand et al. 1987, Michael 1988).

Most other elements show moderately poor to no correlation with Si or the *Ba-group* (Table 4, Fig. 5). However, among these elements

a third group can be distinguished which show high positive mutual correlation coefficients, that is Zr, Hf, Lu, Yb and Ta (R = +0.91 to +0.63) Table 4, Fig. 7). Also Tb and Th show relatively good positive correlations with the elements in this group which is called the *Zr-group*. The highest positive correlation coefficients in this group are found for those elements which have the highest partition coefficients (PC) zircon/melt (using data by Mahood & Hildreth 1983, Fujimaki 1986 and Lemarchand et al. 1987). (Hf: R = +0.79, PC$\geq$ 1000; Lu: R = +0.83, PC = 600-700; Yb: R = +0.74, PC$\approx$ 500; Th: R = +0.54, PC = 60-90) (Table 4, Fig. 7). It should be noted that the low correlation coefficients between the elements in the *Zr-group*, and the *Ba-group* and Si, do not result from curved or broken trends, but reflect the same lack of co-variation as is shown by the Zr-SiO_2 plot (Fig. 5).

The strongest positive correlations with Si are found for Rb, U and Cr (R>+0.55) (Table 4, Fig. 5). This group will be referred to as the *Rb-group*. Such a correlation could be explained in terms of low PC mineral/melt (highly likely since all major and accessory phases are believed to have PC << 1 for these elements) and high distribution coefficients melt/vapour.

Discussion and conclusions

Fractional crystallization

Some of the compositional variations observed in the Eikeren ekerite are compatible with partitioning of elements between a silicic melt and minerals crystallizing from that melt (alkali feldspar + sodic amphibole ± acmitic pyroxene + ilmenite + titanomagnetite + apatite). This is true for the elements in the *Ba-group* (Ba, Eu, Ca, Sm, Na, P, Mg, Al and Ti) which show strong positive correlations with each other and strong negative correlations with Si (Table 4, Fig. 7). We also interpret the strong positive correlations between Sc and Ca-Na-Ti to reflect high partition coefficients amph/melt, (cpx/melt) and sphene/melt. The behaviour of elements in the *Zr-group* also appears to be governed by mineral/melt partitioning.

Fractional crystallization can, however, by no means explain all the compositional variations in the Eikeren ekerite. The lack of correla-

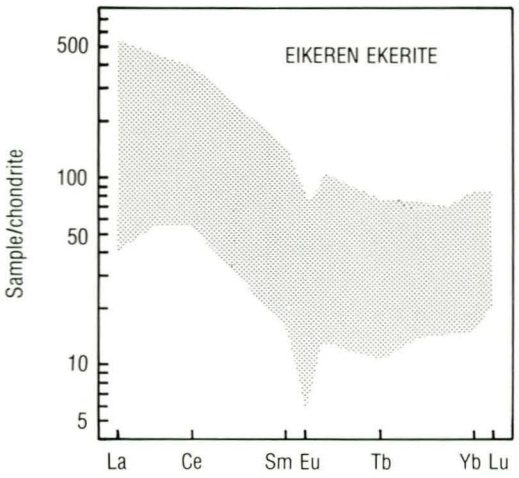

Fig. 6. Range of chondrite-normalized rare earth element patterns in the Eikeren ekerite, based on 23 analyzed samples (Table 3).

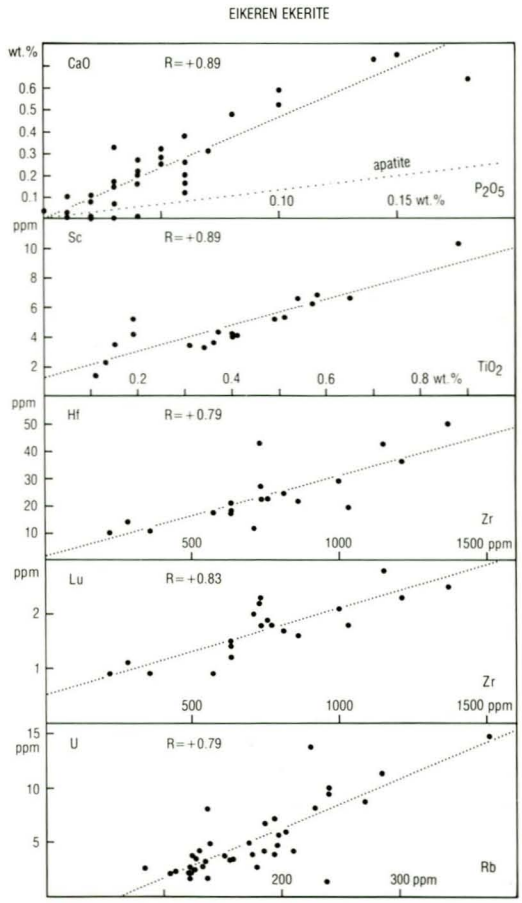

Fig. 7. Examples of element — element relations discussed in the text. R= correlation coefficient (see explanation in the text). Also shown are estimated linear regression trends.

tions seen among many of the elements (R close to 0) is the typical result of a combination of processes. It should be noted that moderate to poor correlations are also observed between elements in the *Ba-group* and other elements which are preferentially picked up by the main magmatic phases: V, La, Mn, Fe, Tb and heavy REE (Table 4). It is concluded that the compositional variations in the Eikeren ekerite are controlled by two or more processes, one of which is fractional crystallization. Other processes which must be considered are fluid transfer, contamination and multiple intrusions of chemically distinct magmas.

Contamination, multiple intrusion

Available evidence suggests that contamination has not affected the Eikeren ekerite on a large scale. Seventeen samples from different parts of the pluton define an isochron in the Rb-Sr isotopic system (Rasmussen et al. 1988). The samples defining the isochron have less than 50 ppm Sr; contamination should therefore be easily detected. However, the secondary reactions discussed above suggest some exchange of CO_2-rich fluids between the Eikeren complex and the countryrocks at subsolidus temperatures.

Several of the plutonic complexes in the Oslo Rift are formed by multiple intrusions of magmas of slightly different compositions due to fractionation processes at different depths in the crust. Examples are the Larvik monzonitic complex (Neumann 1980) and the Glitrevann granitic stock (Jensen 1985). It has, however, not been possible to subdivide the Eikeren granite into separate intrusive units on the basis of field, petrographic or compositional criteria. The poor correlations observed among many of the elements in the Ekeren complex cannot therefore be attributed to multiple intrusion processes.

F and Cl in fluid and melt

Fluid inclusion studies have revealed that a saline fluid was involved in the formation of the Eikeren ekerite complex. Hansteen & Burke (1990) have presented a model for the evolution of this fluid phase:

- The supersolidus magmatic fluids carried large amounts of dissolved salts, 55-70 weight % NaCl-equivalents and are best described as hydrosaline melts. The content of CO_2 (or other C-O compounds) was low.
- At subsolidus temperatures the salinity decreased gradually, and late hydrothermal fluids contained mainly Na, K and Cl. Considerable amounts of CO_2-rich fluids separated from the bulk fluid through subsolidus boiling processes.
- In addition, late CO_2-rich fluid inclusions are found in some samples.

It will be shown below that interaction between melt, minerals and fluid may account for the compositional variations observed in the Eikeren ekerite, and that fluid transport continued at subsolidus temperatures.

Whereas fluid inclusion studies indicate that the supersolidus fluid was rich in Cl, mineral chemical data (high concentrations of F, and Cl below the detection limit in amphibole, apatite and biotite) indicate quite high F/Cl ratios in the coexisting ekerite magma. Manning et al. (1980, 1984) and Candela (1986) have shown that when a vapour phase is evolved, Cl is strongly partitioned into the vapour (V) whereas F is retained in the silicic melt (l) ($D_{Cl}^{V/l}$= 40-50, $D_F^{V/l}$ = 0.2—0.3). The separation of a free fluid phase will therefore be recorded in minerals like apatite and amphibole as marked increases in the F/Cl ratio. The Eikeren amphiboles and apatites show high, constant F/Cl ratios. This must mean that the Eikeren ekerite was already vapour-saturated at the time of intrusion into its present position.

A rough positive correlation between F-concentration in amphibole and bulk rock SiO_2 (Fig. 3) suggests that the bulk distribution coefficient mineral/melt, $D_F^{s/l}$, was below unity. According to Kovalenko et al. (1984) this may well be the case in F-rich systems as $D_F^{s/l}$ decreases as C_F^l increases. At a late stage of fractionation the ekeritic melt became, at least locally, saturated in CaF_2.

The pattern of decreasing F-content from core to rim observed in amphiboles in some samples is not consistent with the general trend of increasing F described above. These amphiboles also show a strongly decreasing Ca-content from core to rim. A likely explanation for this discrepancy is that the rims of these amphiboles equilibrated at subsolidus temperatures with a fluid that had deposited fluorine in interstitial fluorite due to decreasing solubility of fluorine in the fluid phase with decreasing temperature (see also Hansteen & Burke 1990). The fluid may also have become increasingly diluted through mixing with meteoric water.

Distribution of elements between silicic melt and fluid

The variations in elements in the *Ba-group* appear to have been governed primarily by melt-crystal partitioning, implying that their melt/fluid distribution coefficients were high. Other elements which preferentially enter the same mineral phases (V, La, Mn, Fe, Tb and heavy REE) show moderate to poor correlations with the elements in the *Ba-group* and must have been significantly affected by fluid transport.

The described differences in the crystallization sequence of the pyriboles, and presence or absence of sphene, suggest that local equilibria were established which differed slightly in physical conditions (such as oxygen fugacity). This in turn can have given rise to small differences in the way each element was distributed between different phases.

Knowing that the magmatic fluid contained 55-70 weight % NaCl-equivalents, and had a high Na/K ratio (Andersen et al. 1990, Hansteen & Burke 1990), it seems some what surprising that the behaviour of Na, in contrast to K, is so consistent with that of the other elements in the *Ba-group*. The explanation may be that the melt stayed saturated in sodium, being buffered by feldspar, pyriboles and fluid. Potassium, on the other hand, was also mobilized during sericitization of the feldspar. It is likely that also the near constant ratio $(Na/K)_{melt}$ (1) irrespective of Si, is the result of partitioning of Na, K and Al between melt, fluid and mineral phases. Experimental work on granitic systems has shown that the (Na+K)/(Si+Al) partitioning between a melt and the coexisting fluid is controlled by the major complexing anions present (B, Cl, F, etc) (e.g. Dingwell & Scharpe 1983). The increasing agpaitic index with increasing SiO_2 in the melt is therefore expected primarily to occur before a free fluid phase is established.

Most of the other elements appear to have been mobile during the crystallization process, including the *Zr-group* which show good correlations between elements which preferentially enter zircon, but poor correlations with other elements. This strongly suggests that the system was open to the elements in the *Zr-group* during crystallization. The bulk rock analyses consequently mainly reflect those amounts of *Zr-group* elements which were trapped in zircon at different stages of crystallization in different parts of the magma chamber, and thus prevented from being transported to other parts of, or out of, the system. The elements in the *Zr-group* must thus have formed complexes which were stable in the fluid phase. It has been well established that in a silicic melt - Cl-rich vapour system, Zr, REE, Ti and Sc are partitioned into the melt, whereas Cu, Pb, Fe, Zn, Cs and Rb enter the Cl-rich fluid (e.g. Alderton et al. 1980, Malinin & Khitarov 1980, Webster & Holloway 1980). However, in the presence of a fluorine-rich fluid phase, elements like Zr and REE will form F-complexes such as ZrF_6^{2+} and LaF_2^+ and LaF_3 (Alderton et al. 1980). This will stabilize these elements in a F-rich solution, and may render them mobile. The Eikeren ekerite appears to be an excellent example of a system where Zr, Hf, Th, Ta and REE were mobilized in a fluid as F-complexes.

The presence of zircon, monazite, niobates and other rare minerals in the ekerite indicates, furthermore, that the silicic melt eventually became saturated in Zr, light REE and Nb. Melt/fluid distribution coefficients for Zr, and light REE must consequently have been slightly above 1.

The relatively strong increase in *Rb-group elements* with increasing SiO_2 (Fig. 5) implies control by melt/fluid distribution coefficients well above 1. This apparent partitioning of Rb into the melt is not expected from experimental studies of silicic melt/vapour systems (e.g. Malinin & Khitarov 1980, Webster & Holloway 1980). However, Bailey & Macdonald (1975) have reported that in the Eburru obsidians (Kenya Rift), which formed in the presence of a vapour phase and which were Zr-undersaturated, Rb correlates with Zr and F rather than with Cl, Nb and Y. The trace elements Ni, Zn and Co appear to have been most mobile.

Subsolidus processes

A variety of secondary reactions and phases deposited along secondary healed fractures show that H_2O-rich fluids continued to pass through the system at subsolidus temperatures. These fluids transported elements like Fe, Na, K, Al and F, possibly also Si.

The above discussion documents how combined mineral-melt, melt-fluid and mineral-fluid fractionation have controlled the different major and trace elements in the Eikeren ekerite. The discussion furthermore shows that, when

combined with methods such as detailed petrography and fluid inclusion studies, an element correlation matrix is a very useful tool for understanding the details of a complex petrogenetic evolution.

Acknowledgements
We are indebted to H. Austrheim, H. Hagen, B.B. Jensen, M. Vadset and T. Winje for assistance with the analyses. We also wish to thank B.B. Jensen for constructive criticism of this manuscript. This study was financed by the Norwegian Council for Technical and Scientific Research (NTNF) through project 621.5.

References

Alderton, D.H.M., Pearce, J.A. & Potts, P.J. 1980: Rare earth element mobility during granite alteration: evidence from southwest England. *Earth Planet. Sci. Lett. 49,* 149–165.

Andersen, T. 1981: *En geokjemisk - petrologisk undersøkelse av de intrusive bergartene i Sande Cauldron, Oslofeltet.* Cand. real. thesis, University of Oslo, 319 pp.

Andersen, T. 1984: Hybridization between larvikite and nordmarkite in the Oslo Region, S. E. Norway: A case study from the Sande cauldron central pluton. *Nor. Geol. Tidsskr. 64,* 221–233.

Andersen, T., Rankin, A.H. & Hansteen, T.H. 1990: Melt-mineral-fluid interaction in peralkaline silicic intrusions in the Oslo Rift, SE Norway. III: Alkali geothermometry based on bulk fluid inclusion content. *Nor. geol. unders. Bull. 417,* 33–40.

Bailey, D.K. & Macdonald, R. 1975: Fluorine and chlorine in peralkaline liquids and the need for magma generation in an open system. *Min. Mag. 40,* 405–415.

Barberi, F., Santacrose, R. & Varet, J. 1982: Chemical aspects of rift magmatism. *In* Palmason, G. (ed.), *Continental and Oceanic Rifts.* Am. Geophys. Union, Geodynamics Series 8, 223–258.

Barth, T.F.W. 1945: Studies on the igneous rock complex of the Oslo Region. II. Systematic petrography of the plutonic rocks. *Skr. Norske Vidensk.-Akad. i Oslo, I. Mat.-naturv. Kl. 1944, No 9,* 104 pp.

Brøgger, W.C. 1890: Die Mineralien der Syenitpegmatitgänge der südnorwegischen Augit- und Nephelinsyenite. *Zeitschr. Krystallogr. Mineralog. 16,* 663p.

Brøgger, W.C. 1906: Eine Sammlung der wichtigsten Typen der Eruptivgesteine des Kristianiagebietes nach ihre geologischen Verwandtschaftsbeziehungen geordnet. *Nyt. Mag. f. Naturv. 44,* 117–144.

Brøgger, W.C. & Schetelig, J. 1926: Geological map of Kongsberg, 1:100 000. *Nor. geol. unders.*

Brunfelt, A.O. & Steinnes, E. 1969: Instrumental activation analysis of silicate rocks with epithermal neutrons. *Anal. Chim. Acta 48,* 13–24.

Candela, P.A. 1986: Toward a thermodynamic model for the halogens in magmatic systems: An application to melt-vapor-apatite equilibria. *Chem. Geol. 57,* 289–301.

Charles, R.W. 1972: Phase equilibria of the richterite end members Na2CaFe5SiO22(OH)2 and Na2CaFe5SiO22-(OH)2. *Carnegie Inst. Wash. Yearbook 71,* 506–510.

Charles, R.W. 1973: The phase equilibria of intermediate compositions on the pseudo-binary richterite - ferrorichterite. *EOS 54,* 478.

Dietrich, R.V., Heier, K.S. & Taylor, S.R. 1965: Studies on the igneous rock complex of the Oslo Region. XX. Petrology and geochemistry of ekerite. *Skr. Norske Vidsk.-Akad., Oslo. I. Mat.-naturv. Kl. Ny Serie No 19,* 31 pp.

Dingwell, D.B., & Scharfe, C.M. 1983: Major element partitioning in the system haplogranite-HF-H2O: implications for leucogranites and high-silica rhyolites (abstr.). *EOS 64,* 342.

Ernst, W.G. 1976: *Petrologic phase equilibria.* Freeman & Co., 322 pp.

Fujimaki, H. 1986: Partition coefficients of Hf, Zr, and REE between zircon, apatite, and liquid. *Contrib. Mineral. Petrol. 94,* 42–45.

Gordon, G.C., Randle, K., Goles, G.G., Corliss, J.B., Beeson, M.H., & Oxley, S.S. 1968: Instrumental activation analysis of standard rocks with high- resolution gamma-ray detectors. *Geochim. Cosmochim. Acta 32,* 369–396.

Govindaraju, K. 1984: 1984 compilation of working values for 170 international reference samples of mainly silicate rocks and minerals. *Geostandard Newsletter VIII (Special Issue),*

Hansteen, T.H., & Burke, E.A.J. 1990: Melt-mineral-fluid interaction in peralkaline silicic intrusions in the Oslo Rift, SE Norway. II: High-temperature fluid inclusions in the Eikeren-Skrim complex. *Nor. geol. unders. Bull, 417,* 15–32.

Jensen, I.S. 1985: Geochemistry of the central granitic stock in the Glitrevann cauldron within the Oslo rift, Norway. *Nor. Geol. Tidsskr. 65,* 201–216.

Kovalenko, V.I., Antipin, V.S., Kovalenko, N.I., Ryabchikov, I.D., & Petrov, L.L. 1984: Fluorine distribution coefficients in magmatic rocks. *Geochim. Int. 21,* 66–84.

Lemarchand, F., Villemant, B., & Calas, G. 1987: Trace element distribution coefficients in alkaline series. *Geochim. Cosmochim. Acta 51,* 1071–1081.

Mahood, G., & Hildreth, W. 1983: Large partition coefficients for trace elements in high–silica rhyolites. *Geochim. Cosmochim. Acta 47,* 11–30.

Malinin, S.D., & Khitarov, N.I. 1980: Base–metal and petrogenetic elements in a magma–fluid system. *Geochim. Int. 21,* 93–103.

Manning, D.C.A., Hamilton, D.L., Henderson, C.M.B., & Dempsey, M.J., 1980: The probable occurrence of interstitial Al in hydrous, F-bearing and F-free aluminosilicate melts. *Contrib. Mineral. Petrol. 75,* 257–262.

Manning, D.C.A., Martin, J.S., Pichavant, M. & Henderson, C.M.B. 1984: The effect of F, B and Li on melt structures in the granite system: Different mechanisms? *In* C.M.B. Henderson (ed.) *Natural Environment Research Council: Progress in Experimental Petrology.* Sixth progress report of research supported by NERC 1981–1984, 36–41.

Michael, P.J. 1988: Partition coefficients for rare earth elements in mafic minerals of high silica rhyolites: The importance of accessory mineral inclusions. *Geochim. Cosmochim. Acta 52,* 275–282.

Neumann, E.-R. 1974: The distribution of Mn2+ and Fe2+ between ilmenites and magnetites in igneous rocks. *Am. J. Sci. 274,* 1074–1088.

Neumann, E.-R. 1976: Compositional relations among pyroxenes, amphiboles and other mafic phases in the Oslo Region plutonic rocks. *Lithos 9,* 85—109.

Neumann, E.-R. 1980: Petrogenesis of the Oslo Region larvikites and associated rocks. *J. Petrol. 21,* 498—531.

Neumann, E.-R., Brunfelt, A.O., & Finstad, K.G. 1977: Rare earth elements in some igneous rocks in the Oslo rift, Norway. *Lithos 10,* 311—319.

Raade, G. 1969: Minerals from the Permian biotite granite at Nedre Eiker Church. *Nor. Geol. Tidsskr. 49,* 227—239.

Raade, G. 1972: Mineralogy of miarolitic cavities in the plutonic rocks of the Oslo Region, Norway. *Mineral. Rec. 3,* 7—11.

Raade, G. 1973: *Distribution of radioactive elements in the plutonic rocks of the Oslo region.* Cand. real. thesis, University of Oslo, 162 pp.

Raade, G., & Haug, J. 1980: Rare fluorides from a soda granite in the Oslo Region, Norway. *Mineral. Rec. 11,* 83—91.

Rae, D.A. & Chambers, A.D. 1988: Metasomatism in the North Qoroq centre, South Greenland: cathodoluminescence and mineral chemistry of alkali feldspar. *Trans. Royal Soc. Edinburgh: Earth Sci. 79,* 1—12.

Ramberg, I.B. 1976: Gravity interpretation of the Oslo Graben and associated igneous rocks. *Nor. geol. unders. 325,* 193 pp.

Rasmussen, E., Neumann, E.-R., Andersen, T., Sundvoll, B., Fjerdingstad, V., & Stabel, A. 1988: Petrogenetic processes associated with intermediate and silicic magmatism in the Oslo rift, southeast Norway. *Min. Mag. 52,* 293—307.

Schuiling, R.D., & Vink, B.W. 1967: Stability relations of some titanium-minerals (sphene, perovskite, rutile, anatase). *Geochim. Cosmochim. Acta 31,* 2399—2411.

Sundvoll, B. 1978: Rb/Sr relationship in the Oslo igneous rocks. *In* Neumann, E.-R. & Ramberg, I.B. (eds.) *Petrology and Geochemistry of Continental Rifts.* D.Reidel, Hingham, Mass., 181—184.

Webster, E.A., & Holloway, J.R. 1980: The partitioning of REE's, Sc, Rb and Cs between a silicic melt and a Cl fluid. *EOS 61 (abstr.),* 1152.

Wörner, G., Beusen, J.-M., Duchateau, N., Gijbels, R. & Schmincke, H.-U. 1983: Trace element abundances and mineral/ melt distribution coefficients in phonolites from the Laacher See volcano (Germany). *Contrib. Mineral. Petrol. 84,* 152—173.

Manuscript received November 1988; revised typescript May 1989; accepted July 1989.